







## Prediction of the response to antiangiogenic sunitinib therapy by non-invasive hybrid diffuse optics in renal cell carcinoma: supplement

**MIGUEL MIRELES,<sup>1,2,†</sup>  GABRIELA JIMÉNEZ-VALERIO,<sup>2,†</sup> **JORDI MORALES-DALMAU,<sup>1</sup> JOHANNES D. JOHANSSON,<sup>1,3</sup>  MAR MARTÍNEZ-LOZANO,<sup>4</sup> ERNESTO E. VIDAL-ROSAS,<sup>1,5</sup>  VALENTÍ NAVARRO-PÉREZ,<sup>6</sup> DAVID R. BUSCH,<sup>7</sup>  ORIOL CASANOVAS,<sup>4</sup> TURGUT DURDURAN,<sup>1,8</sup>  AND CLARA VILCHES<sup>1,\*</sup> ****

<sup>1</sup>*ICFO - Institut de Ciències Fotòniques, The Barcelona Institute of Science and Technology, 08860 Barcelona, Spain*

<sup>2</sup>*Computational Optics and Translational Imaging Lab, Northeastern University, Boston, Massachusetts 02115, USA*

<sup>3</sup>*Department of Biomedical Engineering, Linköping University, SE-581 83 Linköping, Sweden*

<sup>4</sup>*Tumor Angiogenesis Group, ProCURE, Catalan Institute of Oncology - IDIBELL, 08908 L'Hospitalet de Llobregat, Spain*

<sup>5</sup>*Digital Health and Biomedical Engineering, School of Electronics and Computer Science, University of Southampton, SO17 1BJ Southampton, UK*

<sup>6</sup>*Clinical Research Unit, Institut Català d'Oncologia, 08908 L'Hospitalet de Llobregat, Spain*

<sup>7</sup>*University of Texas Southwestern Medical Center, Departments of Anesthesiology and Pain Management, Neurology, and Biomedical Engineering Dallas, Texas 75390-9003, USA*

<sup>8</sup>*ICREA - Institució Catalana de Recerca i Estudis Avançats, 08010 Barcelona, Spain*

<sup>†</sup>*These authors contributed equally to this work*

\**clara.vilches@icfo.eu*

---

This supplement published with Optica Publishing Group on 6 September 2024 by The Authors under the terms of the [Creative Commons Attribution 4.0 License](https://creativecommons.org/licenses/by/4.0/) in the format provided by the authors and unedited. Further distribution of this work must maintain attribution to the author(s) and the published article's title, journal citation, and DOI.

Supplement DOI: <https://doi.org/10.6084/m9.figshare.26830069>

Parent Article DOI: <https://doi.org/10.1364/BOE.532052>

**PREDICTION OF RESPONSE TO ANTIANGIOGENIC SUNITINIB THERAPY BY NON-INVASIVE HYBRID DIFFUSE OPTICS IN RENAL CELL CARCINOMA:  
SUPPLEMENTAL DOCUMENT**

<b>Tumor</b>	<b>Control</b>	<b>Treated</b>	<b>Statistics</b>
THC [ $\mu\text{M}$ ]	$68 \pm 35$	$47 \pm 30$	$p < 0.01$
SO <sub>2</sub> [%]	$74 \pm 11$	$70 \pm 9$	$p = 0.01$
BFI [ $10^{-8}\text{cm}^2\text{s}^{-1}$ ]	$3 \pm 2$	$2 \pm 1$	$p < 0.01$

<b>Shoulder</b>	<b>Control</b>	<b>Treated</b>	<b>Statistics</b>
THC [ $\mu\text{M}$ ]	$40 \pm 8$	$40 \pm 8$	$p = 0.87$
SO <sub>2</sub> [%]	$54 \pm 5$	$54 \pm 6$	$p = 0.71$

**Table S1.** Mean values  $\pm$  standard deviation for THC, SO<sub>2</sub> and BFI for the whole treatment period, in tumor and shoulder positions, for treated (n = 22) and control animals (n = 13).

<b>Group</b>	<b>log(THC)</b>	<b>log(SO2)</b>	<b>log(BFI)</b>
Responder – non-responder	0.17	0.21	0.01 (*)
Responder – control	0.77	0.20	0.88
Non-responder – control	0.46	0.77	0.09

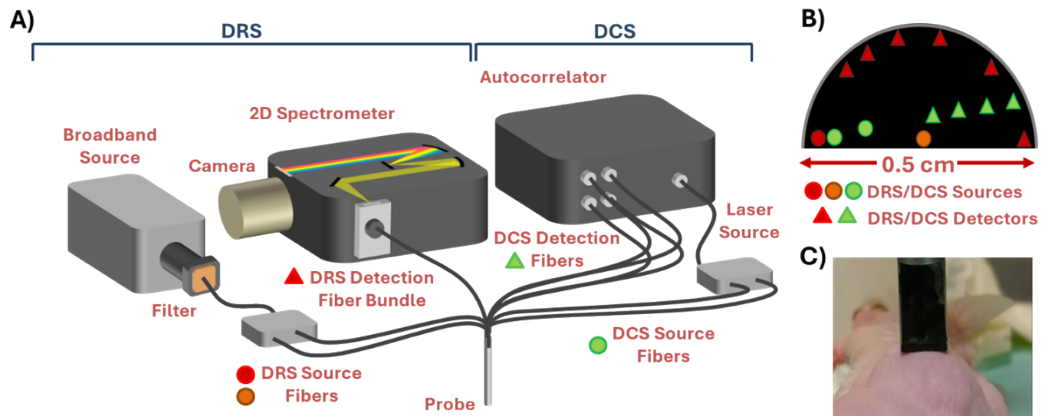
**Table S2.** Summary of pre-treatment tumor hemodynamics statistics (p values) among therapy outcomes. n = 13 controls, 8 non-responders, 14 responders.

<b>Univariate analysis</b>	<b>AUC</b>	<b>p</b>	<b>P<sub>bs</sub></b>
THC	0.68	0.15	$\square$ 0.07
SO <sub>2</sub>	0.68	0.14	$\square$ 0.07
BFI	0.81	0.01	$\leq$ 0.03

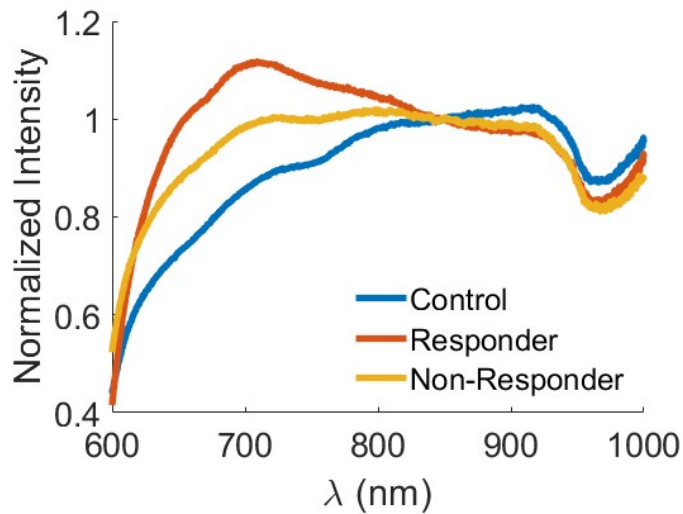
  

<b>Multivariate analysis</b>	<b>AUC</b>	<b>p</b>	<b>P<sub>bs</sub></b>
THC & BFI	0.79	0.047	$\leq$ 0.049
THC & SO <sub>2</sub>	0.67	0.320	$\square$ 0.190
BFI & SO <sub>2</sub>	0.79	0.052	$\square$ 0.050

**Table S3.** Pre-treatment therapy outcome classification by binomial logistic regression.



**Figure S1.** The hybrid DRS/DCS device. **A.** An illustration of the optical components of the hybrid DRS/DCS setup. **B.** A schematic of the tip of the contact hand-held probe composed of a set of fibers for light delivery (red/orange dots for DRS and green dots for DCS) and collection (red triangles for DRS and green triangles for DCS) into and from the tissue. **C.** A representative image of the probe placement on the tumor.



**Figure S2.** Example data of the calibrated optical measurements acquired at day 6 of treatment from the right-side of the tumor of a representative mouse in each of the therapy outcome groups (Control, Responder and Non-Responder) at 0.46 cm source-detector separation. Optical data was normalized at 850 nm for scaling purposes. Spectral shape differences reflect the complex interplay of the optical data due to heterogeneous tumor constituents.

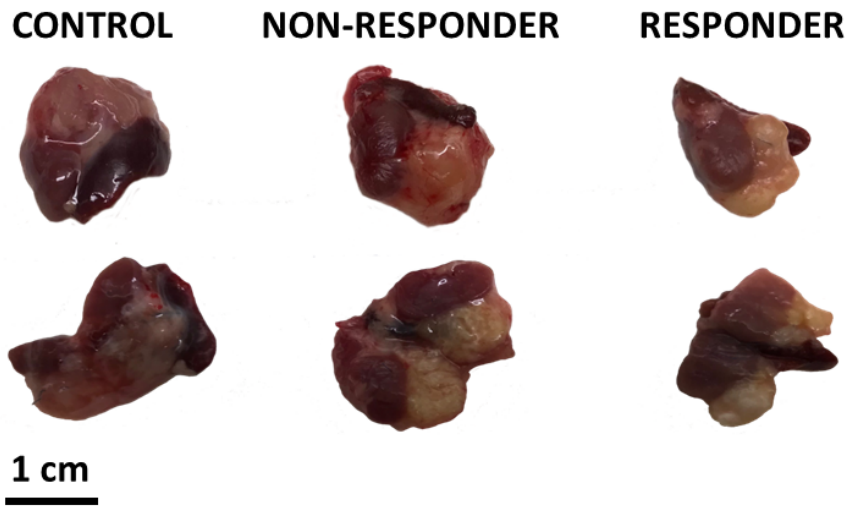


**Figure S3.** Representative images of control, responder and non-responder tumors at end point.

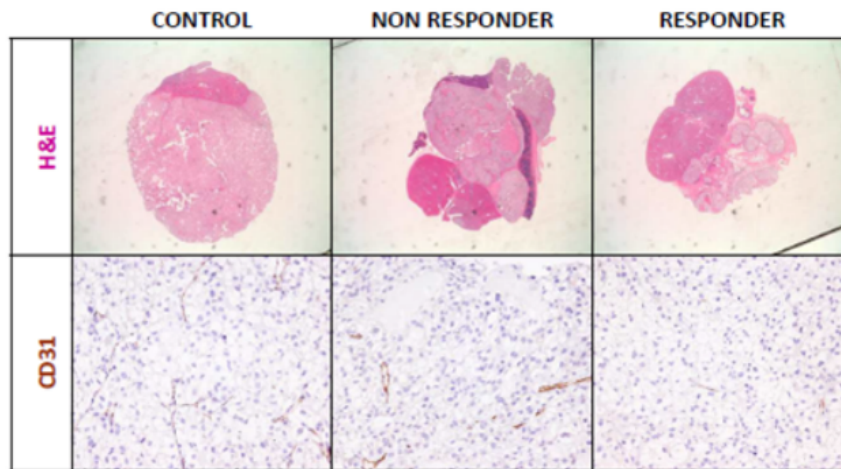


**Figure S4.** Representative images of hematoxylin and eosin stained tissue to quantify necrotic tumor areas (upper row) and immunohistochemical staining of CD31 to assess microvessel density (20x, bottom row).